Mutational Analysis of Loops 1 and 5 of the Hairpin Ribozyme[†]

Richard Shippy, Andrew Siwkowski, and Arnold Hampel*

Department of Biological Sciences, Northern Illinois University, DeKalb, Illinois 60115

Received August 26, 1997; Revised Manuscript Received November 3, 1997

ABSTRACT: A comprehensive analysis of base preferences for all positions in loops 1 and 5 of the hairpin ribozyme−substrate complex was carried out using a *cis*-ribozyme tethered to substrate by a pentapyrimidine loop. Ribozyme−substrate molecules were mutated to contain each of the three non-native base variations at each of the eight positions within these loops. Catalytic activity was measured for each mutant and compared to the activity of the original native sequence. This was the first time all base positions in these loops have been mutated to all variants and kinetically characterized. Various effects were found, ranging from invariant base positions to those with nearly complete tolerance of any base change. Two positions resulted in cleavage rates below the lower limit of accurate quantification for all non-wild-type base substitutions. These positions are G_8 in the ribozyme and G_{s6} in the substrate. When A_{10} was substituted with a pyrimidine, self-cleavage activity fell below the lower limit of detection while the remaining positions showed varying base preferences. The information reported here on loops 1 and 5 combined with previous mutagenesis data on loops 2 and 4 [Siwkowski, A., Shippy, R., and Hampel, A. (1997) *Biochemistry 36,* 3930−3940] completed a comprehensive mutational/kinetic analysis of every base position located within all the required loops of the hairpin ribozyme−substrate complex and allowed for the development of a mechanism for catalysis which is proposed.

The hairpin ribozyme was derived from the catalytic core of the minus strand of the satellite RNA from tobacco ringspot virus [(−)sTRSV][1] (*1*). Hairpin ribozymes are a class of RNA enzymes (*2*) capable of site-specific and reversible transesterification cleavage reactions on RNA substrates (*1*). The hairpin ribozyme is capable of cleaving in either a *cis* or a *trans* reaction (*3*, *4*), yielding products with 5′-hydroxyl and 2′,3′-cyclic phosphate termini (*5*). Three other classes of naturally occurring ribozymes, the hammerhead, hepatitis delta, and *Neurospora* ribozymes, also produce these cleavage products (*6*). The minimal sequence of the hairpin ribozyme and substrate necessary for catalysis is 50 and 14 ribonucleotides, respectively (*4*). When the ribozyme is bound with substrate, the secondary structure (Figure 1) consists of five loops, loops 1, 2, 3, 4, and 5, separated by four helices, helices 1, 2, 3, and 4 (*7*, *8*). A recently identified noncanonical A-G base pair in helix 4 extended the known number of base pairs in the structure to 18 bp (*9*, *10*). Two of the helices (helices 1 and 2) are formed between the substrate and ribozyme, resulting in two symmetrical loops directly across from each other (loop 1 in the ribozyme and loop 5 in the substrate). The remaining three loops are found within the ribozyme region as a result of helix 3 and helix 4 formation. The only loop within the ribozyme−substrate complex not required for catalytic activity is loop 3. It can be removed to form a bimolecular ribozyme with kinetic properties similar to the one-piece ribozyme (*11*), or it can be replaced by a more stable tetraloop RNA structure to increase activity (*12*). The hairpin ribozyme−substrate complex likely folds into a three-dimensional structure using A_{15} as a hinge (*13*, *14*), allowing bases in loops 2 and 4 to interact with bases in loops 1 and 5. The existence or nature of additional interactions between these four loops is at present unknown.

Understanding the structure−function of the hairpin ribozyme has practical applications since the hairpin ribozyme has been effective against HIV-1 *in vivo* (*15*). Determining the structure−function relationship of the hairpin ribozyme may be valuable for improving its catalytic activity and likewise improving its efficacy as a genetic therapeutic agent. To date, structure−function information on the hairpin ribozyme has been based on phylogenetic comparisons, mutational studies, *in vitro* selection, cross-linking, NMR, and chemical modification data.

The study reported here is the first to kinetically analyze every base in loops 1 and 5 for cleavage. Substitutions at two positions resulted in cleavage rates below the lower limit of accurate quantification. These are G_8 in the ribozyme and G_{s6} in the substrate. When A_{10} was substituted with a pyrimidine, self-cleavage activity fell below the lower limit of detection. The information reported here on loops 1 and 5, combined with previous mutagenesis data on loops 2 and 4 by Siwkowski et al. (*9*), provides a comprehensive analysis of possible base interactions between these loops as well as the identification of invariant positions which may be involved in the catalytic step itself. This study completed a comprehensive mutational/kinetic analysis of every base

[†] Supported by NIH Grant R01AI29870 to A.H.

* To whom correspondence should be addressed.

[1] Abbreviations: (−)sTRSV, negative strand of the satellite RNA of tobacco ringspot virus; (−)sCYMV1, negative strand of the satellite RNA 1 of chicory yellow mottle virus; (−)sArMV, negative strand of the satellite RNA of arabis mosaic virus; FS, full size autocatalytic RNA; 3′P, 3′ cleavage product; 5′P, 5′ cleavage product.

S0006-2960(97)02128-4 CCC: $15.00
Published on Web 01/13/1998

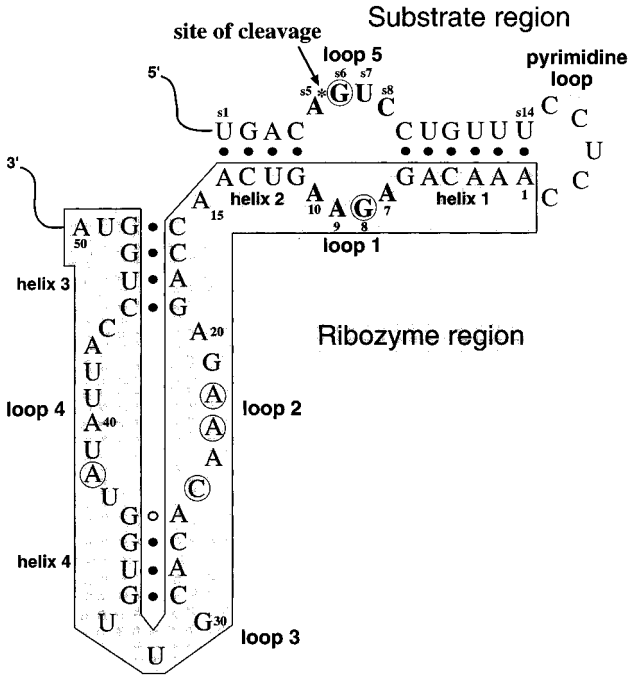

FIGURE 1: *cis*-Cleaving hairpin ribozyme−substrate two-dimensional model. The model contains four helical regions (helices 1, 2, 3, and 4) and five single-stranded loop regions (loops 1, 2, 3, 4, and 5). This model includes a noncanonical A_{26}-G_{36} base pair at the end of helix 4 (*9*). The catalytic core consists of a 50-nucleotide ribozyme strand (shaded region) and a 14-nucleotide substrate strand. Cleavage occurs between A_{s5} and G_{s6} in loop 5 of the substrate. The construct used in these studies linked the substrate to the ribozyme with a pentapyrimidine loop (CCUCC). The six circled bases represent positions which, when changed, resulted in no detectable cleavage.

located within all the required loops of the hairpin ribozyme−substrate complex. A mechanism for catalysis is proposed.

MATERIALS AND METHODS

The cis-Cleaving Hairpin Ribozyme−Substrate Construct. The construct used in these studies was the *cis*-cleaving ribozyme−substrate complex (Figure 1) (*9*, *16*). Site-directed mutagenesis was performed on each base in loops 1 and 5.

Loops 1 and 5 Mutagenesis. The following PCR primers were used in generating coding DNA for loop 1 and loop 5 mutants:

Loops 1 and 5 Conserved Primer:
5'-GGTATCGATAAGCTTGCATGCCTGCAGGTCGACTACCAGGTAA TATACCACAACGTGTGTTTCTCTGGTTGAC-3'

Loop 1 Mutagenesis Primers:

A_7: 5'-GAACTAGTGGATCCTTTTTTTTTTTTTTGACAGTCCTGTTTCCTCC AAACAGNGAAGTCAACCAGAGAAACACACGTTGTGG-3'

G_8: 5'-GAACTAGTGGATCCTTTTTTTTTTTTTTGACAGTCCTGTTTCCTCC AAACAGANAAGTCAACCAGAGAAACACACGTTGTGG-3'

A_9: 5'-GAACTAGTGGATCCTTTTTTTTTTTTTTGACAGTCCTGTTTCCTCC AAACAGAGNAGTCAACCAGAGAAACACACGTTGTGG-3'

A_{10}: 5'-GAACTAGTGGATCCTTTTTTTTTTTTTTGACAGTCCTGTTTCCTCC AAACAGAGANGTCAACCAGAGAAACACACGTTGTGG-3'

Loop 5 Mutagenesis Primers:

A_{s5}: 5'-GAACTAGTGGATCCTTTTTTTTTTTTTTGACNGTCCTGTTTCCTCC AAACAGAGAAGTCAACCAGAGAAACACACGTTGTGG-3'

G_{s6}: 5'-GAACTAGTGGATCCTTTTTTTTTTTTTTGACANTCCTGTTTCCTCC AAACAGAGAAGTCAACCAGAGAAACACACGTTGTGG-3'

U_{s7}: 5'-GAACTAGTGGATCCTTTTTTTTTTTTTTGACAGNCCTGTTTCCTCC AAACAGAGAAGTCAACCAGAGAAACACACGTTGTGG-3'

C_{s8}: 5'-GAACTAGTGGATCCTTTTTTTTTTTTTTGACAGTNCTGTTTCCTCC AAACAGAGAAGTCAACCAGAGAAACACACGTTGTGG-3'

Mutagenesis was carried out as previously described by Siwkowski et al. (*9*). In summary, double-stranded DNA fragments were synthesized using PCR by extension of primer dimers, each containing a randomized base corresponding to the eight base positions found in loop 1 (A_7−A_{10}) and loop 5 (A_{s5}−C_{s8}) of the hairpin ribozyme−substrate complex. These randomized positions are represented as **N** in the loop 1 and loop 5 mutagenesis primers. The primers were randomized individually during DNA synthesis using an equimolar phosphoramidite mix containing only the non-wild-type bases. The double-stranded DNA containing the mutations was digested with *Bam*HI and *Hin*dIII and cloned into the pL2GMC vector in place of the wild-type sequence (Figure 2). Sequencing identified each of the clones representing three non-wild-type variants at each base position and also verified the integrity of the remaining ribozyme−substrate coding sequences. In this manner, 3 different non-wild-type mutants were obtained for each of the 8 positions in loops 1 and 5, resulting in a panel of 24 mutant clones.

Kinetic Analysis. Kinetic analysis was performed as described previously by Siwkowski et al. (*9*). Briefly, each clone was linearized with *Hin*dIII and transcribed with T7 RNA polymerase using [α-^{32}P]CTP to produce internally labeled autocatalytic RNA. During transcription, aliquots were taken at 20, 40, and 60 min and transcription (cleavage) products separated on a denaturing polyacrylamide gel. RNA was detected using autoradiography, bands corresponding to full-size RNA and those corresponding to the 3′ product were excised and counted, and the rates of self-cleavage were determined by nonlinear regression analysis of the resulting time-course data using the equation:

$$\text{uncleaved fraction} = [(1 - b)(1 - e^{-kt})/kt] + b$$

The term k is the unimolecular rate constant for self-cleavage (min^{-1}) and b is the fraction of full-size RNA produced unable to undergo self-cleavage.

The kinetic data obtained from these curve fits provided information on appropriate incubation times for the next series of transcription reactions, in order to more accurately determine the catalytic parameters of each mutant relative to wild-type. A second set of transcription reactions was conducted in the same manner as previously described, but instead, five aliquots were taken during a total incubation time of either 15, 30, or 60 min. These five time points were used in nonlinear regression analysis as above to determine the catalytic parameters of each mutant. The resulting rates of self-cleavage for each mutant were compared to wild-type to determine relative effects of base mutations on rates of self-cleavage.

RESULTS AND DISCUSSION

The *cis*-cleaving hairpin ribozyme (Figure 1) had each base position in loops 1 and 5 mutated to contain all non-wild-type base moieties. The pL2GMC construct (Figure 2) was used for the construction of a panel of clones representing every base possibility at each individual position within loops 1 and 5. Transcription/cleavage reactions of the mutant clones as well as the wild-type construct (Figure 3) showed one position in each the ribozyme and substrate where cleavage rates were below the lower limit of accurate

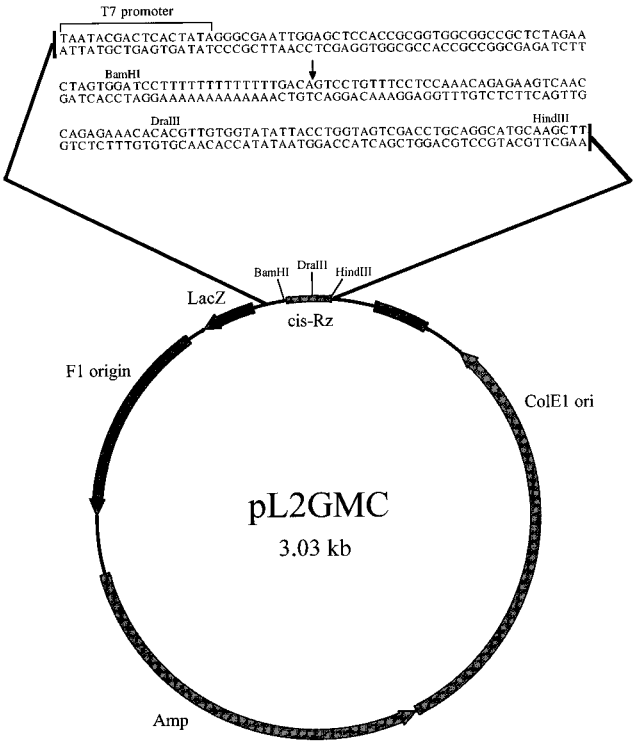

FIGURE 2: Construct pL2GMC codes for the wild-type *cis*-cleaving ribozyme−substrate complex. The restriction sites *Bam*HI and *Hin*dIII were used for cloning of the loop 1 and loop 5 mutants.

quantification for all three non-wild-type base substitutions. These positions were G_8 in the ribozyme and G_{s6} in the substrate. Pyrimidine substitutions at A_{10} also resulted in levels of cleavage below the accurately determinable level. A_7 and A_{s5} accommodated all base possibilities while retaining near-wild-type levels of self-cleavage activity. Other positions showed varying degrees of tolerance with regard to base substitutions.

Nonlinear regression analysis of cleavage using the equation:

$$\text{uncleaved fraction} = [(1 - b)(1 - e^{-kt})/kt] + b$$

determined the unimolecular rate constant (k) for self-cleavage. This was then compared to wild-type (k_{wt}/k_{mut}) (Figure 4, Table 1). The b-values (uncleavable fractions) were near zero for each mutant and therefore not included in Table 1.

A detailed description of the results for each base position follows.

Loop 1 Ribozyme Positions A_7−A_{10}

A_7. This position is variable since no more than a 6× reduction in self-cleavage rate accompanied the incorporation of any mutant base at this position. A_7U and A_7C resulted in 3.8× and 5.6× reductions in self-cleavage activity, respectively. The guanine substitution in this position decreased catalytic activity by approximately 2×. Based on these results, a purine is preferred in this position. This purine bias could be due to the stabilization of helices when purines are the last unpaired base on the 3′ end of a helix (*17*).

These results are contrary to those previously published from *in vitro* selection, where the active-pool variants A_7U and A_7C retained 100% relative self-cleavage activity while A_7G exhibited 80% relative self-cleavage activity compared to wild-type (*18*). In a previous *trans*-cleavage experiment, A_7G and A_7C retained wild-type activity (*8*). When *cis*- and *trans*-acting systems were compared, the A_7C mutation resulted in a 54% reduction in *cis*-cleavage activity while this same mutation retained full activity in a *trans* reaction (*19*). This result is in agreement with the catalytic activity recorded for A_7C in our *cis*-cleaving construct relative to the published *trans* results. In contrast to the self-cleaving construct of Berzal-Herranz et al. (*18*), where the 5′ end of the substrate is tethered to the 3′ end of the ribozyme, the self-cleaving construct of Fujitani et al. (*19*) has the 3′ end of the substrate tethered to the 5′ end of the ribozyme, in the same manner as in our experiments. Overall, it appears this position is variable in both *cis*- and *trans*-acting systems. It is likely A_7 does not serve a necessary structural role and is not involved in the catalytic step.

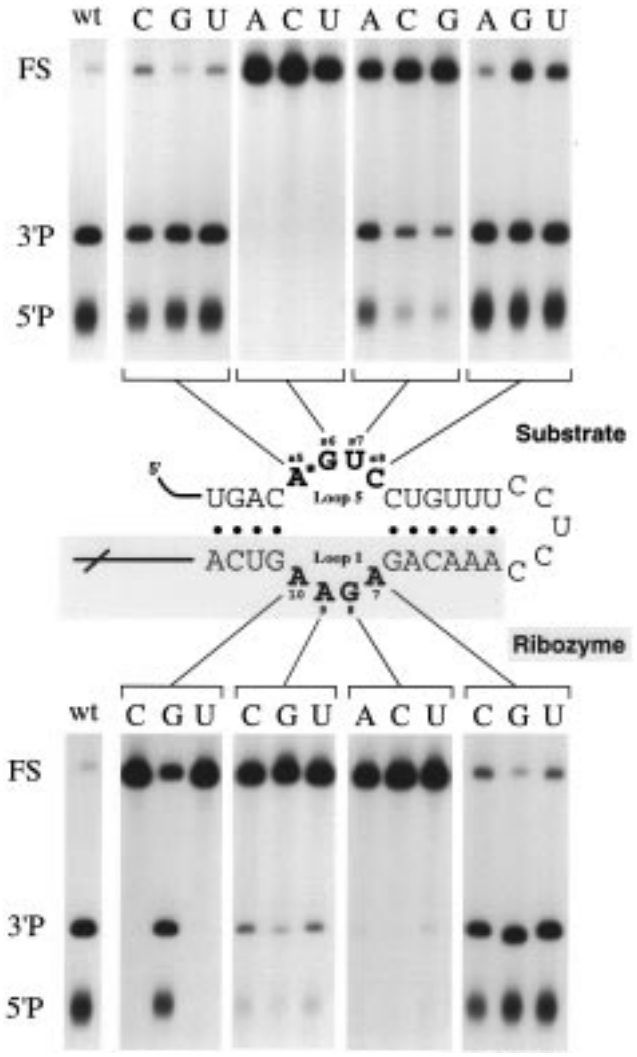

FIGURE 3: Self-cleavage analysis of the hairpin ribozyme−substrate catalytic RNA. Each panel represents a particular position in either loop 1 or loop 5. The base at each position was mutated to contain each of the three non-wild-type bases. Linearized plasmids were transcribed for 60 min to permit both transcription and cleavage of the RNA. Reaction products were separated on 10% PAGE, denaturing 7 M urea gels. FS, full-size ribozyme−substrate RNA; 3′P, the 3′ cleavage product; 5′P, the 5′ cleavage product; wt, the wild-type self-cleaving ribozyme−substrate RNA.

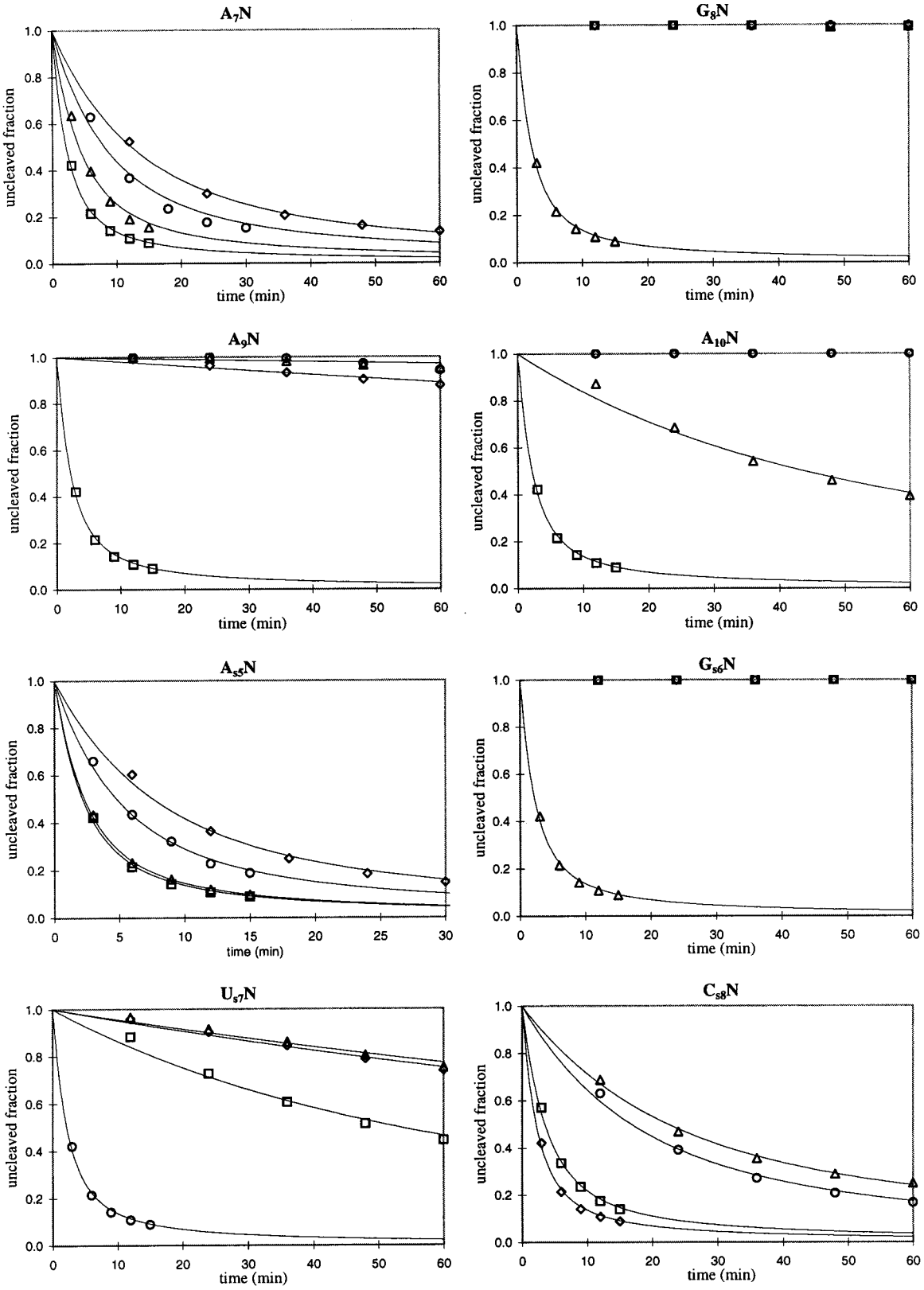

FIGURE 4: Self-cleavage kinetics of loop 1 and loop 5 hairpin ribozyme−substrate mutants. Each graph represents the uncleaved fraction of self-cleaving RNA as a function of time. Each line represents a different base substitution for that position in the *cis*-cleaving ribozyme−substrate complex. □ = A, △ = G, ◇ = C, ○ = U.

G8. This was the only position in loop 1 of the ribozyme where cleavage rates were below the lower limit of accurate quantification for all mutants. Mutating this position corresponded to a decrease in catalytic activity of greater than 1200×. This was the first time all three non-wild-type base substitutions at G_8 were tested for self-cleavage activity.

G_8C and G_8U mutants gathered from an inactive pool of ribozyme variants, obtained from *in vitro* selection, showed less than 1% self-cleavage activity while the G_8A mutant was never obtained nor assayed for self-cleaving activity. However, G_8A and G_8U mutants in a *trans*-cleavage assay strongly inhibited activity (*18*). A previous *trans*-cleavage

Table 1: Kinetic Analysis of Loop 1 and Loop 5 Mutants[a]

nat base	mutation	k (min^{-1})	k_{wt}/k_{mut}
	Loop 1 Mutants		
wt	none	0.73 (±0.06)	−
A_7	C	0.12 (±0.01)	5.6
	G	0.38 (±0.05)	1.9
	U	0.19 (±0.04)	3.8
G_8	A	<0.0006	>1200
	C	<0.0006	>1200
	U	<0.0006	>1200
A_9	C	0.0041 (±0.0008)	182
	G	0.0014 (±0.0006)	730
	U	0.001 (±0.003)	730
A_{10}	C	<0.0006	>1200
	G	0.036 (±0.006)	18
	U	<0.0006	>1200
	Loop 5 Mutants		
wt	none	0.73 (±0.06)	−
A_{s5}	C	0.21 (±0.02)	3.5
	G	0.69 (±0.03)	1.1
	U	0.33 (±0.03)	2.2
G_{s6}	A	<0.0006	>1200
	C	<0.0006	>1200
	U	<0.0006	>1200
U_{s7}	A	0.030 (±0.004)	24
	C	0.010 (±0.001)	73
	G	0.009 (±0.001)	73
C_{s8}	A	0.45 (±0.03)	1.6
	G	0.074 (±0.004)	10
	U	0.095 (±0.009)	7.3

[a] The lower limit of detection for k was 0.0006/min.

study reported no cleavage activity for the G_8C mutant, while G_8U retained 5% cleavage activity relative to wild-type (*8*). In a base modification study using a three-piece ribozyme−substrate construct, catalytic activity decreased by approximately 98% when either the exocyclic amino group, N^7, or N^1-H of G_8 was removed (*20*). Increased concentrations of Mg^{2+} partially restored activity for both the inosine and O^6-methylguanosine substitutions, suggesting possible magnesium coordination at the exocyclic amino group and the N^1 hydrogen atom of G_8 (*20*). Removal of the N^7 group from G_8 increased K_M by 5×. Based on dramatic protection of G_8 from kethoxal in a ground-state structure, it has been suggested this base may form a direct contact with loop 5, possibly through a noncanonical base pair, or it may be involved distally in a tertiary interaction with a portion of the ribozyme in either loop 2 or loop 4 (*21*). Also, results obtained from NMR implicate a possible cross-strand interaction between the base of G_8 and the sugars of both G_{s6} and U_{s7} in the ground-state structure (*22*). In a previous study, A_{s5} in loop 5 of the substrate cross-linked primarily to G_8 (*23*), providing evidence for a cross-strand interaction between these two loops and the possible involvement of G_8 in this sort of interaction. In any case, G_8 plays a critical role in the catalytic step and/or the formation of the active ribozyme−substrate complex.

A_9. This position does not require adenine for self-cleavage, but this base is strongly preferred. All mutations at this position resulted in nearly complete loss of activity. The A_9G and A_9U mutations decreased self-cleavage activity 730× while A_9C had a 182× decrease in catalytic activity. This position can accommodate any of the three non-wild-type bases and still support self-cleavage, albeit at low levels.

A_9 has been reported as being essential (*18*). Reactions in *trans* of an A_9U mutation resulted in no detectable cleavage (*8*). In *trans* reactions, removal of the exocyclic amino group or N^7 from this position resulted in an 8-fold or 21-fold decrease in k_{cat}, respectively (*20*). It has been proposed magnesium binds to the N^7-position of A_9 in the transition state, based on a restoration of near-wild-type activity, with N^7-deazaadenosine in this position, at high magnesium concentrations. The A_9G mutation decreased self-cleavage activity 730×, and since the N^7 group is retained, it is likely A_9 contributes more than just the N^7 group for the formation of the active tertiary structure. Since the conservation of adenine at this position is not a requirement for self-cleavage, A_9 is likely not directly involved in the catalytic step but may coordinate with a metal or other bases for proper folding. A_9 is a highly critical base for the formation of the catalytically active tertiary conformation.

A_{10}. This position must be a purine in order for the ribozyme to retain cleavage activity. The G mutation resulted in an 18× decrease in cleavage activity. However, either pyrimidine mutation resulted in cleavage rates below the accurately determinable level, corresponding to decreases in catalytic activity greater than 1200×.

Removal of the exocyclic amino group or N^7 from this position resulted in a 16× and 8× reduction in k_{cat}, respectively (*20*). A_{10} was reported to be required for ribozyme activity based on an *in vitro* selection, since all mutations at this position were not recovered from an active pool of ribozyme variants (*18*). In a *trans*-cleavage assay, $A_{10}G$ supported 61% relative catalytic activity compared to wild-type (*8*). Since the retention of a purine at this position appears to be necessary for self-cleavage, the purine backbone itself is likely involved in a key structural and/or catalytic role. It is possible the N^3 group of A_{10} may be involved in this key role. Interestingly, the crystal structure of a group 1 ribozyme domain shows examples of functional group coordination involving both the N^3 and 2′-hydroxyl groups of adenosine (*24*). Since the 2′-hydroxyl of A_{10} was shown to be essential for catalytic function (*25*), coordination involving both the N^3 and 2′-OH groups at this position cannot be ruled out as a structural motif.

Loop 5 Substrate Positions A_{s5}−C_{s8}

A_{s5}. This position is completely variable. No more than approximately a 3× reduction in self-cleavage rate accompanied any mutation in this position. The $A_{s5}G$ mutant retained nearly full activity, while the $A_{s5}C$ had the lowest activity, indicating a purine is preferred in this position. Base preferences at this position, based on relative decreases in self-cleavage activity, show the same order as would be predicted based on thermodynamic stability. Unpaired terminal ribonucleotides at the end of a helix, with the same structural context as A_{s5}, have the lowest free energy when purines occupy this position while cytidine at this position has the highest free energy (*17*).

Substrate cleavage by the hairpin ribozyme, in a *trans* reaction, was unchanged for any base in this position (*7*, *26*). However, these earlier studies did not measure kinetic

rates. These results show A_{s5} is not involved in key catalytic or structural interactions.

G_{s6}. This was the only base position in the substrate loop where cleavage rates were below the lower limit of accurate quantification for any of the three non-wild-type base substitutions. These results support the original observation in *trans*-cleavage assays wherein unmodified base changes at this position completely eliminated catalytic activity (*7*, *8*, *26*).

A 2-aminopurine substitution at this position maintains near-wild-type catalytic activity while an inosine substitution abolishes activity (*26*). Therefore, it has been proposed that the exocyclic amino group on G_{s6} is an essential component of the active site required for catalysis, while the keto group is not involved in cleavage. Substitutions at G_{s6} with either inosine or O^6-methylguanosine resulted in cleavage rates too slow to be measured, and removal of the N^7 group resulted in a 80-fold reduction in k_{cat}, while K_M was unaffected (*20*). Based on significantly increased values for K_{Mg}(app) with the N^7-deazaguanosine substitution, Grasby et al. (*20*) proposed magnesium binds to the N^7 group of G_{s6} in the ground state. Based on these base modification results, N^7 is not required for cleavage. In contrast, the exocyclic amino group appears to be required while the functional group requirement of the N^1-hydrogen atom cannot be ruled out.

The results of our self-cleavage study support the base modification studies, since each of the nonmodified base mutations at this position eliminates a required functional group, which likewise abolishes catalytic activity. It has also been proposed, based on an NMR ground-state structure, that A_9 and G_{s6} form a cross-strand-sheared A-G base pair (*22*). In any case, the conservation of G_{s6} is a requirement since this base clearly plays a key structural and/or catalytic role.

U_{s7}. Uridine at this position greatly facilitates but is not required for self-cleavage. When U_{s7} was changed to either C or G, cleavage activity decreased 73×. U_{s7}A resulted in a 24× reduction in catalytic activity. This was the first time kinetic rates of cleavage were obtained for any mutation at this position. These results are consistent for *trans*-cleavage reactions, where U_{s7}C and U_{s7}G resulted in approximately 1% and 2% cleavage, respectively, while U_{s7}A showed 7% cleavage activity relative to wild-type (*8*). Psoralin cross-linking experiments showed possible tertiary interactions between U_{s7} and ribozyme residues in loop 4 of the ground-state structure (*27*). It has been proposed, based on an NMR ground-state structure, that the residues on either side of U_{s7} are splayed apart. This places U_{s7} in the expanded major groove without interacting with the other positions in loop 5 (*22*). The conformational flexibility and lack of steric hindrance of uracil may allow tertiary contacts between loop 5 and other regions of the ribozyme without inducing major conformational changes in the substrate loop. Conformational changes resulting from base substitutions at U_{s7} greatly reduce, but do not eliminate, cleavage activity. Since this position can support cleavage for all non-wild-type base substitutions, in both *cis*- and *trans*-cleavage assays, it is likely U_{s7} has no direct involvement in the cleavage step, but is favored for formation of the transition-state structure.

C_{s8}. Cytidine is not required at this position to support near-wild-type levels of self-cleavage. When this position was changed to adenine, it retained nearly full catalytic activity. However, when the C_{s8}G and C_{s8}U mutations were made, catalytic activity decreased by 10× and 7.3×, respectively. The *cis*-reaction gave somewhat different results than those previously obtained in *trans*. In *trans*-cleavage reactions, C_{s8}U had the highest catalytic activity for all non-native base substitutions (*2*, *8*, *26*). The mutations C_{s8}U retained 25% relative cleavage activity while C_{s8}A and C_{s8}G resulted in cleavage activities of 2% and 1% compared respectively to wild-type (*8*). Using *trans*-acting ribozymes, decreases in k_{cat} were approximately 9× for C_{s8}A, 8× for C_{s8}U, and 36× for C_{s8}G (*2*). However, the catalytic efficiencies for ribozymes containing these mutations were 180×, 30×, and 180× lower than wild-type, respectively, as a result of large increases in the K_M values. It is clear that differences exist between *cis* and *trans* systems when non-native base substitutions are introduced at C_{s8}. This is consistent with the observation of Fujitani et al. (*19*) where the C_{s8}A mutation is fully active in *cis* but retained 58% activity relative to wild-type in *trans*. Base substitutions at this position likely interfere with the substrate-binding step in *trans*-cleavage reactions. In our *cis*-cleaving construct, and the construct of Fujitani et al. (*19*), the substrate strand is transcribed first followed by a six base pair helix 1, which may stabilize and promote the formation of the active ribozyme−substrate complex.

Phylogenetic comparisons of the three naturally occurring hairpin ribozymes [from (−)sTRSV, (−)sCYMV1, or (−)-sArMV] showed either an A or a C at this position in loop 5 directly across from either a C or a A, respectively, in loop 1 (*2*). The optimal combination at these positions may be the conservation of an A/C pair. The double mutation of A_7C/C_{s8}A significantly increased the low C_{s8}A cleavage activity in a *trans*-cleavage assay (*8*). Furthermore, the double mutation of A_7C/C_{s8}A increased the cleavage activity of the A_7C mutation (*19*). These compensatory mutational data from *trans*-cleavage assays, combined with the phylogenetic conservation of these opposing bases, suggest a possible interaction between these base moieties. Phylogenetic conservation is favored at position C_{s8} since C_{s8}A retained wild-type self-cleavage activity. A favorable interaction may occur when an A/C pair is retained in the *trans*-cleaving system. Therefore, this possible interaction is not required for the catalytic step but may facilitate substrate recognition or binding.

Mechanism Proposed for Cleavage

The classic model of RNA cleavage is that of bovine pancreatic RNase A. Its mechanism involves a transesterification reaction pathway where deprotonation of the 2′-hydroxyl leads to an in-line nucleophilic attack of the resulting oxyanion on the neighboring phosphorus. A trigonal bipyramid intermediate is formed as a result of this attack (*28*). The 5′-oxygen−phosphorus bond is cleaved following protonation of the 5′-oxyanion leaving group. The resulting cleavage products have 5′-hydroxyl and 2′,3′-cyclic phosphate termini. These same cleavage products have been identified for the hairpin ribozyme (*5*).

A similar cleavage mechanism is supported for the hairpin ribozyme (Figure 5). The hairpin ribozyme can utilize the inert transition metal complex cobalt hexaammine [$Co(NH_3)_6^{3+}$] in the cleavage mechanism, indicating that,

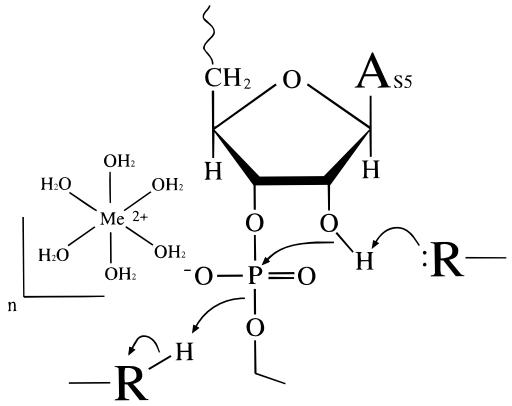

FIGURE 5: Mechanism of cleavage for the hairpin ribozyme. The mechanism of cleavage is likely a simple stabilization of the transition state by functional groups required in the RNA sequence itself; there is no direct involvement of a metal for the cleavage step itself.

unlike other ribozymes, direct binding of the metal cofactor to phosphate oxygen is not required for catalytic activity (*29*, *30*). Efficient cleavage of R_p- and S_p-phosphorothioate substrate analogs in both Mg^{2+} and $Co(NH_3)_6^{3+}$ buffers further supports this model (*29*, *30*). In RNase A, the developing negative charge during transesterification is neutralized by the positively charged side group of a lysine residue (*31*). This role may be served in the haipin ribozyme by the positively charged metal−aquo complex. The role of the two histidines in the RNase A cleavage mechanism may be served by the base functional groups within the hairpin ribozyme itself. His-12, which has a pK_a value of 6.4, serves as the general base catalyst by deprotonating the 2′-hydroxyl. His-119, which has a pK_a value of 6.8, serves as the general acid catalyst by protonating the 5′-oxyanion leaving group.

Functional groups on RNA purines and pyrimidines have acid−base properties which may be able to participate in acid−base catalysis in a similar manner to the proposed mechanism of RNase A. However, the pK_a values of functional groups on free ribonucleosides are near 4 and 10. This large separation in pK_a values is an explanation for the nearly independent pH cleavage profile for the hairpin ribozyme between pH 5.5 and 9 (*30*). A nearly independent pH profile would occur for an acid−base cleavage reaction where the separation in pK_a values of functional groups, involved directly in the cleavage mechanism, is outside the pH range tested. The study reported here, combined with that of Siwkowski et al. (*9*), identified six base positions which when mutated resulted in cleavage rates below the lower limit of detection. These positions are G_8, A_{22}, A_{23}, C_{25}, A_{38}, and G_{s6} (circled bases in Figure 1). It is possible that two of these bases are directly involved in the catalytic mechanism.

ACKNOWLEDGMENT

We are grateful to Dr. Richard King and Dr. James Erman for helpful comments during preparation of the manuscript.

REFERENCES

1. Buzayan, J., Gerlach, W., and Bruening, G. (1986) *Nature 323*, 349−352.
2. DeYoung, M. B., Siwkowski, A., Lian, Y., and Hampel, A. (1995) *Biochemistry 34*, 15785−15791.
3. Feldstein, P., Buzayan, J. M., and Bruening, G. (1989) *Gene 82*, 53−61.
4. Hampel, A., and Tritz, R. (1989) *Biochemistry 28*, 4929−4933.
5. Buzayan, J., Hampel, A., and Bruening, G. (1986) *Nucleic Acids Res. 14*, 9729−9743.
6. Long, D., and Uhlenbeck, O. (1993) *FASEB J. 7*, 25−30.
7. Hampel, A., Tritz, R., Hicks, M., and Cruz, P. (1990) *Nucleic Acids Res. 18*, 299−304.
8. Anderson, P., Monforte, J., Tritz, R., Nesbitt, S., Hearst, J., and Hampel, A. (1994) *Nucleic Acids Res. 22*, 1096−1100.
9. Siwkowski, A., Shippy, R., and Hampel, A. (1997) *Biochemistry 36*, 3930−3940.
10. Hampel, A. (1998) in *Progress in Nucleic Acids Research and Molecular Biology, Vol. 58: The Hairpin Ribozyme: Discovery, Two-Dimensional Model and Development for Gene Therapy* (Moldave, K., Ed.) pp 1−39, Academic Press, San Diego.
11. Chowrira, B. M., and Burke, J. (1992) *Nucleic Acids Res. 20*, 2835−2840.
12. Yu, M., Poeschla, E., Yamada, O., DeGrandis, P., Leavitt, M., Heusch, M., Yee, J., Wong-Staal, F., and Hampel, A. (1995) *Virology 206*, 381−386.
13. Feldstein, P., and Bruening, G. (1993) *Nucleic Acids Res. 21*, 1991−1998.
14. Komatsu,Y., Koizumi, M., Nakamura, H., and Ohtsuka, E. (1994) *J. Am. Chem. Soc. 116*, 3692−3696.
15. Welch, P., Hampel, A., Barber, J., Wong-Staal, F., and Yu, M. (1996) in *Nucleic Acids and Molecular Biology, Vol 10: Catalytic RNA* (Eckstein, F., and Lilley, D. M. J., Eds.) pp 315−327, Springer, Berlin.
16. Altschuler, M., Tritz, R., and Hampel, A. (1992) *Gene 122*, 85−90.
17. Freier, S. M., Kierzek, R., Jaeger, J. A., Sugimoto, N., Caruthers, M. H., Neilson, T., and Turner, D. H. (1986) *Proc. Natl. Acad. Sci. U.S.A. 83*, 9373−9377.
18. Berzal-Herranz, A., Joseph, S., Chowrira, B. M., Butcher, S., and Burke, J. (1993) *EMBO J. 12*, 2567−2574.
19. Fujitani, K., Sasaki-Tozawa, N., and Kikuchi, Y. (1993) *FEBS Lett. 331*, 155−158.
20. Grasby, J., Mersmann, K., Singh, M., and Gait, M. (1995) *Biochemistry 34*, 4068−4076.
21. Butcher, S., and Burke, J. (1994) *J. Mol. Biol. 244*, 52−63.
22. Cai, Z., and Tinoco, I. (1996) *Biochemistry 35*, 6026−6036.
23. Vitorino Dos Santos, D., Fourrey, J.-L., and Favre, A. (1993) *Biochem. Biophys. Res. Commun. 190*, 377−385.
24. Cate, J. H., Gooding, A. R., Podell, E., Zhou, K., Golden, B. L., Kundrot, C. E., Cech, T. R., and Doudna, J. A. (1996) *Science 273*, 1678−1685.
25. Chowrira, B. M., Berzal-Herranz, A., Keller, C. F., and Burke, J. (1993) *J. Biol. Chem. 268*, 19458−19462.
26. Chowrira, B. M., Berzal-Herranz, A., and Burke, J. (1991) *Nature 354*, 320−322.
27. Monforte, J. A. (1991) Ph.D. Thesis, University of California at Berkeley.
28. Usher, D., Erenrich, E., and Eckstein, F. (1972) *Proc. Natl. Acad. Sci. U.S.A. 69*, 115−118.
29. Hampel, A., and Cowan, J. A. (1997) *Chem. Biol. 4*, 513−517.
30. Nesbitt, S., Hegg, L. A., and Fedor, M. J. (1997) *Chem. Biol. 4*, 619−630.
31. Fersht, A. (1984) *Enzyme Structure and Mechanism*, 2nd ed., W. H. Freeman and Co., New York.

BI9721288